Ocean Engineering 328 (2025) 121040

Contents lists available at ScienceDirect

Ocean Engineering

journal homepage: www.elsevier.com/locate/oceaneng

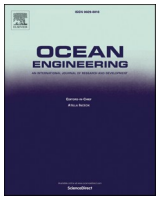

Research paper

Hydrodynamic performance and narrow gap resonance of WEC-floating breakwater hybrid system: An experimental study

Binzhen Zhou [a,b], Chusen Lin [b], Xu Huang [b], Qi Zhang [b], Yuan Yuming [b], Hengming Zhang [c,*], Peng Jin [b,**], Yifeng Yang [d]

[a] State Key Laboratory of Subtropical Building and Urban Science, South China University of Technology, Guangzhou, 510641, China
[b] School of Civil Engineering and Transportation, South China University of Technology, Guangzhou 510641, China
[c] Department of Civil and Environmental Engineering, The Hong Kong Polytechnic University, 999077, China
[d] Department of Mechanical Engineering, University College London, Torrington Place, London WC1E 7JL, United Kingdom

ARTICLE INFO

Keywords:
Floating breakwater
Wave energy converter
Energy conversion efficiency
Wave attenuation
Wave resonance
Model test

ABSTRACT

Wave energy is a significant ocean renewable resource with vast reserves and wide distribution. Integrating a wave energy converter (WEC) and a floating breakwater offers an effective answer to promote its commercialization. In this study, model tests are conducted to investigate the wave energy absorption and attenuation performance of the WEC-breakwater hybrid system with various WEC geometries, focusing on narrow-gap resonance. Optimal configurations for gap width and WEC dimensions were identified. The results reveal a significant improvement in both energy absorption and wave attenuation performance of the WEC-breakwater hybrid system compared to single WEC or single breakwater. Particularly, the hybrid system with an asymmetric triangle-baffle WEC exhibits broader efficiency range frequency and superior wave energy conversion efficiency, while also enhancing the wave reduction capabilities of the floating breakwater for short waves. Effects of the narrow gap resonance on the hybrid systems with symmetric and asymmetric WECs differ. The system with a narrower gap and a slender WEC exhibits better wave energy absorption performance, but the influence on wave attenuation is found to be limited. These findings could provide valuable recommendations for designing WEC-breakwater hybrid systems, helping to avoid unnecessary costs resulting from improper design.

Nomenclature

WEC	Wave Energy Converter
OWC	Oscillating Water Column
OT	Overtopping
OB	Oscillating Body
PTO	Power Take-Off
PIC	Particle-in-Cell
CFD	Computational Fluid Dynamics method
RAO	Response Amplitude Operator
ζ_3	Heave response amplitude operator
H_r	Reflected wave height
H_t	Transmitted wave height
H_i	Incident wave height
K_t	Reflection coefficient
K_t	Transmission coefficient
E_w	Incident wave power

(*continued on next column*)

(*continued*)

P_{ave}	Average wave power
η	Energy conversion efficiency
P_m	Wave power per unit mass
A_ω	Wetted surface of the model
F_{PTO}	PTO damping force
T	Wave period
V	Velocity of the model in heave direction
ω	Frequency of the incident wave
ω_0	Natural frequency of the model in heave direction
b_f	Coefficient of the total friction
c_0	Hydrostatic restoration coefficient
ρ	Density of water
κ	Dimensionless damping
t	Time
M	Mass of floater
L	Length of floater

(*continued on next page*)

This article is part of a special issue entitled: Wave resonance phenomena published in Ocean Engineering.

* Corresponding author.
** Corresponding author.
E-mail addresses: zhanghengminga@163.com (H. Zhang), jinpeng@scut.edu.cn (P. Jin).

https://doi.org/10.1016/j.oceaneng.2025.121040
Received 4 February 2025; Received in revised form 16 March 2025; Accepted 20 March 2025
Available online 28 March 2025

(*continued*)

B	Width of model
D	Draft of model

1. Introduction

As a potential ocean renewable energy source, wave energy is the subject of extensive research (Zhang et al., 2021). However, the commercialization of wave energy faces challenges owing to the high construction costs and low conversion efficiency of wave energy converters (WECs) (Astariz and Iglesias, 2015). An approach of WECs integrating to the offshore structures has been proposed, aiming to reduce power generation costs through cost-sharing, space-sharing, and multi-functionality. This approach is expected to enhance the economy of wave energy utilization and accelerate the process of commercialization (Cheng et al., 2022a). The OB-type WEC is notable for its higher efficiency and ease of integration with floating structures among the overtopping (OT), Oscillating Water Column (OWC), and oscillating body (OB) (Zhou et al., 2023a, 2023b). Meanwhile, floating breakwaters offer extensive applicability for shoreline protection with its flexible design and no demand of supporting structure (McCartney and ASCE, 1985). Due to the similarity and compatibility in the structure and function, hybrid systems of OB-type WECs and floating breakwater in two forms, single-floater and dual-floater hybrid system, have been widely studied (Zhang et al., 2021b).

The single-floater hybrid system is characterized by the direct integration of a power-take-off system (PTO) within the floater, enabling the floater to function both as a floating breakwater and a WEC for power generation (Cheng et al., 2022b). To enhance its performance, the research on the single-floater hybrid system has primarily concentrated on optimizing the shape, size, and PTO system (Zhao et al., 2019b). A single-floater hybrid system composed of a rectangular OB-type WEC and a floating breakwater was proposed to study the effects of PTO damping force and the incident wave height on the performance of wave energy absorption and attenuation through experimental and numerical simulation studies (Ning et al., 2016; Zhao et al., 2017a). Building on their work, Chen et al. (2020) introduced a PIC (Particle-in-Cell) method grounded in viscous fluid theory to further refine the shape of the hybrid system previously proposed by Ning et al. (2016). However, the results indicated that no matter how the shape is optimized, the energy conversion efficiency of a symmetrical hybrid system is inherently limited to 50 %. Therefore, to address the limitations of symmetrical floaters, numerous studies have focused on the development of asymmetrical floaters. Yeung and Madhi et al. (2014, 2018) introduced the Berkeley Wedge, an asymmetrical floater design, which demonstrated a peak energy-capturing efficiency of 96.34 %. Zhang et al. (2020b) proposed a triangle-baffle hybrid system with the maximum energy conversion efficiency of 93 %. Zhou et al. (2024b) then conducted a comparative study of hybrid systems between rectangular and triangular bottoms, both with and without baffles, experimentally confirming that the performance of asymmetrical shape floaters is superior to that of symmetrical ones. This finding was further supported by their subsequent work, where they established a two-dimensional semi-analytical model for an asymmetrical floater and discovered that increasing the asymmetry degree significantly improves the energy extraction performance of the hybrid system (Zhou et al., 2022a, 2023d). Despite these advancements, many previous studies, including those mentioned, indicate that the energy harvesting performance of single-floater hybrid systems remains unsatisfactory in low-frequency waves.

Recognizing the limitation of the single-floater hybrid system, researchers have been motivated to investigate alternative system configurations that can augment the efficacy of wave energy conversion across a more extensive spectrum of wave frequencies. Ning et al. (2017, 2018a, 2018b) demonstrated that the dual-floater hybrid system, composed of two pontoons in tandem, widens the effective frequency range compared to the single-floater system, thus increasing its operational range. In this context, the dual-floater hybrid system has been considered as a promising solution (Mustapa et al., 2017). Considering the synergistic benefits of integrating WEC and floating breakwater, such as the enhancement of WEC power generation performance through the wave-focusing effect of the floating breakwater (Zhou et al., 2022b, 2023e)and cost reduction (He et al., 2013) through shared mooring systems, scholars have concentrated their efforts on this type of hybrid system. Zhao et al. (2017b, 2019a) investigated a rectangular WEC integrating with a floating pontoon-type breakwater, with the PTO system positioned at the top of the WEC. Their results indicated that the wave energy conversion performance of deploying OB-type WECs in front of the floating breakwater is larger than that of a single WEC, owing to the superposition of reflected wave and incident wave. Reabroy et al. (2018), Zhou et al. (2023c), and Martinelli et al. (2016) reached comparable conclusions, highlighting the dual-floater hybrid system exhibits better energy conversion efficiency and wave attenuation performance than that of the single-floater hybrid system, with power amplification of more than 2.5 times. Similarly, scholars have also investigated the symmetry of WEC shapes within dual-floater hybrid systems. Zhang et al. (2020a) adopted the Computational Fluid Dynamics method (CFD) to study the performance of dual-floater hybrid systems incorporating WECs with varying geometries. The results revealed that the dual-floater hybrid system with an asymmetric WEC demonstrated superior wave energy absorption and wave attenuation capabilities compared to that with a symmetric WEC.

Notably, a narrow gap exists between the WEC and the floating breakwater of a dual-floater hybrid system. Under specific hydrodynamic conditions, the oscillatory motion of the fluid within this narrow gap can undergo significant amplification, resulting in heightened wave amplitude and concentrated energy transfer, a phenomenon characterized as narrow gap wave resonance(Zhao et al., 2020). Since the concentration of wave energy within the narrow gap influences the hydrodynamic forces and motion characteristics of the hybrid system, numerous related research has been conducted. Jiang et al. (2018) constructed a two-dimensional numerical model utilizing OpenFOAM to study two side-by-side fixed boxes, finding that the wave forces on the boxes may increase markedly due to wave resonance, which is adverse to the stability and durability of the structures. Mi et al. further emphasized that the heave motion of floaters during resonance can lead to distinct reductions in both horizontal and vertical wave forces, while an increase in upstream structural breadth ratio gradually suppresses normalized peak loads across wave frequencies (Mi et al.,2025; 2025). Furthermore, the wave resonance frequency reduces when the gap width increases (Jiang et al., 2019). Ning et al. (2018b) investigated the wave elevation between two barges, indicating the frequency of narrow gap resonance was related to the barge draft. Following this, Li and Zhang (2016) developed a numerical wave tank based on fully nonlinear potential-flow theory to investigate the influence of gap width on wave resonance, finding that the relative width of the barges significantly influenced the amplitude of the wave surface. In the study of the dual-floater hybrid system, Zhang et al. (2021a) also paid attention to the effect of the narrow-gap resonance phenomenon, noting that the narrow-gap resonance enhances the performance of symmetric WEC while degrading that of asymmetric WEC in the hybrid system. This dynamic interaction is further complicated by floater motions, as free heave motion of adjacent structures alters the resonance patterns and load distributions, suggesting a need to consider combined effects of geometric configurations and body mobility (Gong et al., 2024, 2025). Moreover, Zhang et al. (2021a) indicated that the wave-focusing effect of the floating breakwater is the main reason for the occurrence of narrow gap resonance.

Despite the significant advancements in the aspect of wave energy conversion reflected by the above literature, a systematic analysis comparing the performance of symmetric versus asymmetric WEC in

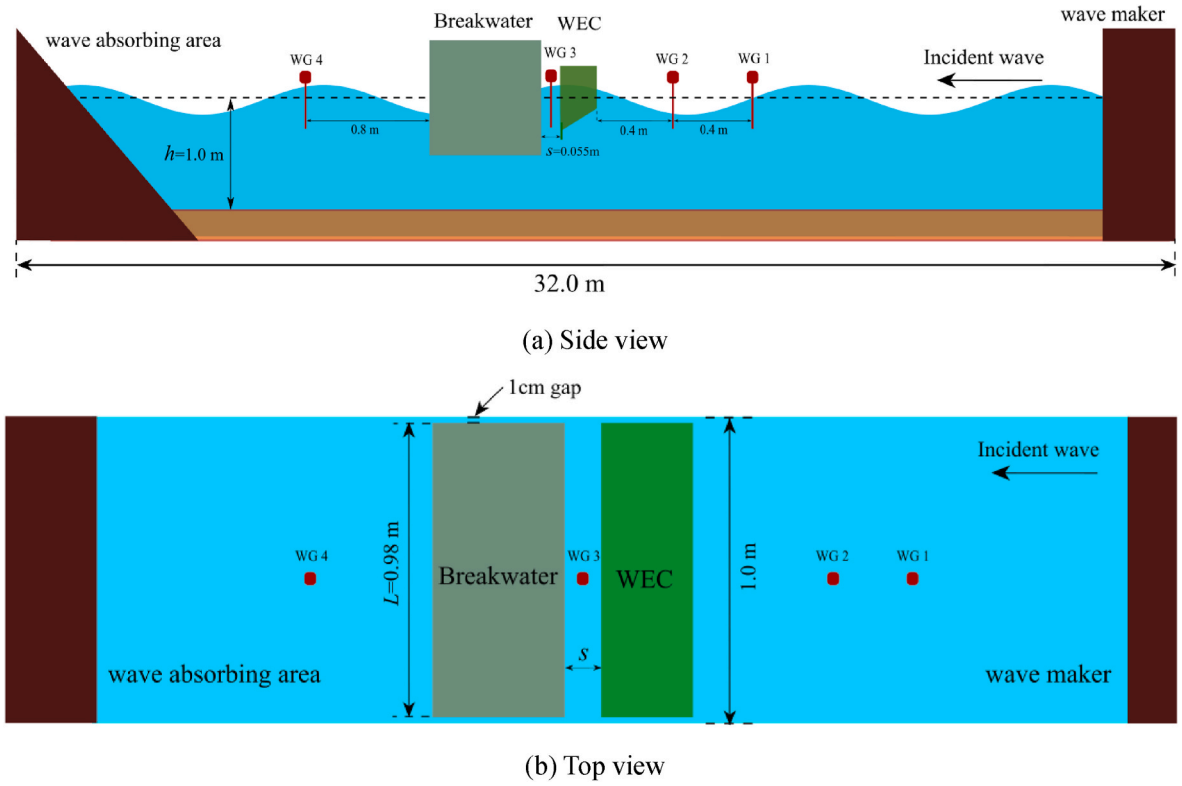

Fig. 1. Configuration of the OB-type WEC-breakwater system in wave flume.

dual-floater systems and the specific impact of narrow gap resonance on system performance is underexplored. The study in this paper focus on comparing the performance of symmetric and asymmetric WEC within the dual-floater hybrid system and demonstrates the superiority of asymmetric WEC in improving wave energy conversion performance. The influence of wave-focusing effects on the narrow gap resonance is clarified, along with its impact on the performance of the dual-floater hybrid systems. The effects of gap width and WEC dimensions on system performance are investigated, providing insights to the design of the WEC-floating breakwater hybrid system. The motivation of the study in this paper is to deeply understand the factors effecting the performance of hybrid systems and to support our findings with experimental data, offering insights and strategies for the advancement of the WEC-breakwater hybrid system.

The paper is structured as follows. Section 2 outlined the experimental setup and the calibration of the experimental system. Moreover, the parameters under investigation are defined and the approach to data analysis is introduced. In Section 3, experimental results are compared with CFD numerical results to verify the accuracy and repeatability of the experiment. In Section 4, the hydrodynamic performance of the dual-floater system is analyzed, aiming to analyze the effects of WEC symmetry, the effects of narrow-gap wave resonance, and the optimization of system dimensions. Section 5 drawn the main conclusions.

2. Experimental setup and calibrations

2.1. Physical model

The WEC-breakwater hybrid system model experiment was conducted in the wave flume laboratory at the School of Civil Engineering and Transportation, South China University of Technology. As depicted in Fig. 1, the size of the wave flume is 32.0 m in length, 1.0 m in width, and 1.5 m in depth. The regular wave periods range of the wave flume is [0.5, 5.0 s], and the maximum wave height is 0.4 m. A wave-absorbing slope is positioned at the left end of the flume to minimize wave reflection. The still water depth has been kept at 1.0 m, and the incident wave propagates from the right hand to the left hand. The experimental model was placed at the midpoint of the wave flume, and the narrow gap

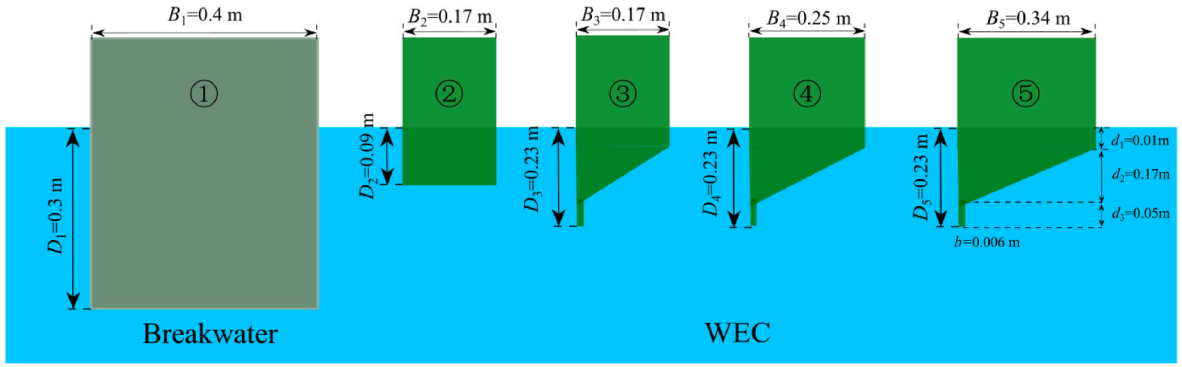

Fig. 2. Dimensions of the WEC and breakwater model.

Table 1
Details of the dimensions of the experimental model.

Model	Geometry	Mass (kg)	Width (m)	Draft (m)
①	Rectangle breakwater	117.6	0.40	0.30
②	Rectangle WEC	14.99	0.17	0.09
③	Triangle-baffle WEC	15.37	0.17	0.23
④	Triangle-baffle WEC	23.72	0.25	0.23
⑤	Triangle-baffle WEC	31.65	0.34	0.23

width S between the WEC and the breakwater was set to 0.055 m. To avoid unnecessary friction and collision, the transverse length L of the experimental models was fixed at 0.98 m, allowing a gap of 1.0 cm to be maintained between each side of the flume wall and the experimental models. Four wave gauges were positioned to measure the wave heights at different locations throughout the experiment.

Considering the capacity of the wavemaker and the wave flume dimension, the scale ratio of the experiment model was set to 1:20 based on Froude similarity. Fig. 2 shows the dimension parameters of these five models involved in this study, including a rectangular breakwater, a rectangular WEC, as well as three triangle-baffle WECs with varying widths. The length of the baffle is $d_3 = 0.05$ m and its thickness is $b = 0.006$ m. Following prior research on the single-floater hybrid system (Zhou et al., 2024b), the ratio of the vertical draft of the triangle-baffle WEC to the draft of its sloped part was set at $d_1{:}d_2 = 1{:}17$. More details of the models can be found in Table 1. The incident wave height H_i is 0.05 m and the range of the wave period T is [0.7, 2.0 s] in the whole experiments.

Fig. 3 depicts the actual experimental model, including both single and dual-floater hybrid systems, along with symmetrical and asymmetrical WECs. The WEC and breakwater models are constructed with acrylic plates, while the fixed frame is made from aluminum alloy profiles. The breakwater model was mounted on a fixed frame and designed for easy disassembly to accommodate various experimental requirements. The motion constraint system, composed of lifting wheels, pulleys, and vertical slide rails, ensures that the WEC moves only in the heave direction, thereby accurately simulating the motion of a heave-type wave energy device. As shown in Fig. 4, the PTO system combined of a gear and a permanent magnet damper, which can provide a

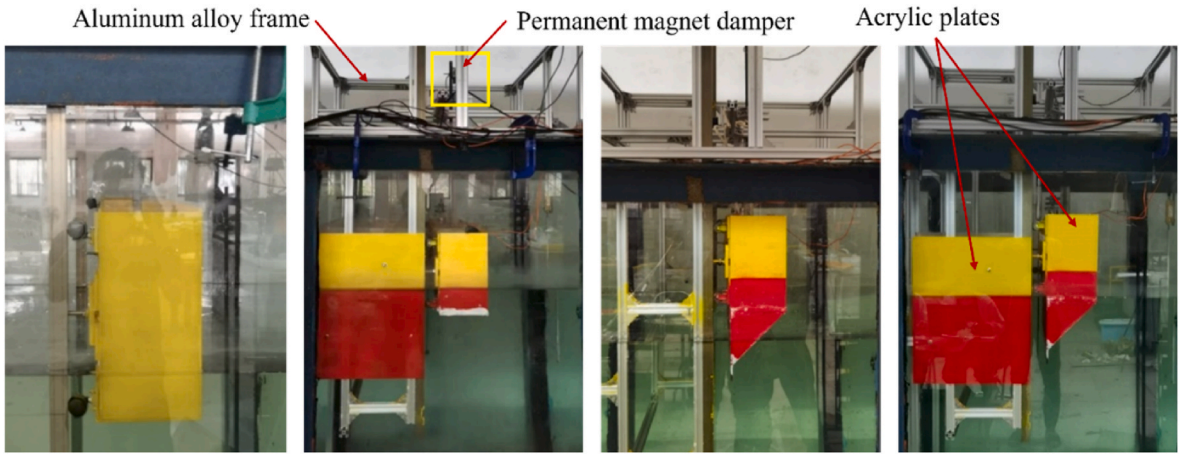

Fig. 3. Photos of the OB-type WEC-floating breakwater hybrid system.

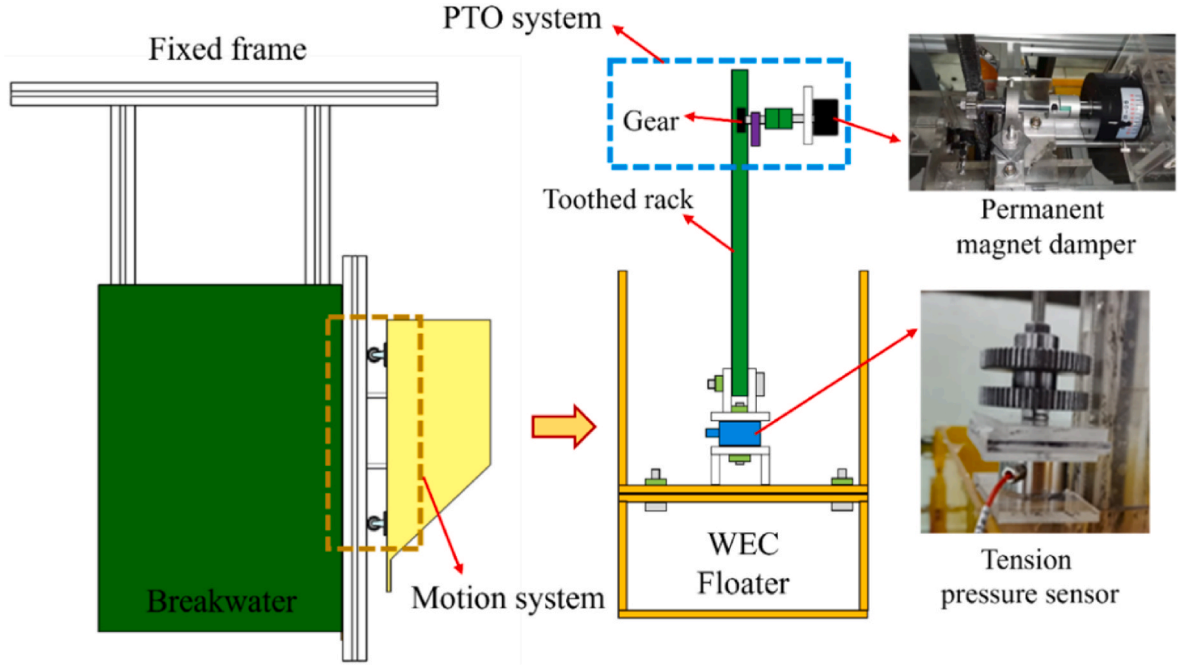

Fig. 4. Details of WEC-breakwater hybrid system model.

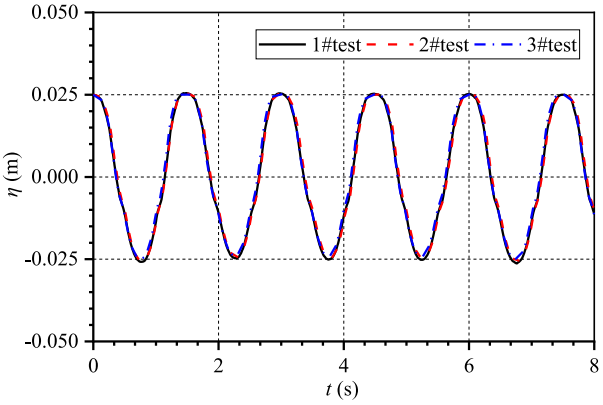

Fig. 5. Time histories of wave surface with $H_i = 0.05$ m and $T = 1.5$ s.

stable damping force. The movement of the WEC drives the connected toothed rack to move and the engagement of the gear with the toothed rack converts the damping torque from the permanent magnet damper into a damping force, which is then measured by a tension pressure sensor fixed between the WEC model and the toothed rack. Additionally, by adjusting the parameters of the permanent magnet damper, different damping forces can be simulated. For a more detailed introduction to the experimental setup, refer to Zhou et al. (2024a,b).

2.2. Experimental system calibrations

2.2.1. Wave calibration

To ensure the accuracy of target wave heights, signal calibration of the wave generation system was conducted. Fig. 5 presents the wave elevation time histories from three repeated tests under conditions of $H_i = 0.05$ m and $T = 1.5$ s. The near-perfect overlap of wave elevation time-history curves confirms waveform consistency and stability of wave-maker, with measured wave heights and periods closely matching target values. The deviation between measured wave heights and theoretical values remained within 5 % across all periods.

2.2.2. Free decay test

Fig. 6 presents the free-decay curves of WEC buoys with different geometric shapes. Through a comparative analysis of experimental measurements and numerical simulation results, the natural period characteristics of each buoy were obtained. Meanwhile, the friction damping coefficients of the buoys were calculated based on Eq. (8) to Eq. (9). The results are systematically summarized in Table 2.

2.3. Data processing

Since the WEC is restricted to move only in the heave direction, the motion amplitude of the WEC model is obtained through a wire displacement sensor. The heave response amplitude operator (RAO) ζ_3 is expressed as the ratio of the WEC motion amplitude A_3 to the incident wave amplitude A_i, where the subscript "3" corresponds to the heave displacement.

$$\zeta_3 = A_3/A_i \tag{1}$$

As shown in Fig. 1, four wave gauges were strategically positioned for dimensionless analysis. Upstream, WG1 and WG2 measured the reflected wave height (H_r) using the two-point method (Goda et al., 1976), WG3 monitored the gap wave height (H_{gap}) between the WEC and breakwater, while WG4 downstream recorded the transmitted wave height (H_t). Three non-dimensional coefficients were established by normalizing measured parameters against the incident wave height (H_i)

$$K_r = H_r/H_i \tag{2}$$

$$K_t = H_t/H_i \tag{3}$$

The incident wave power for an arbitrary water depth can be calculated as follows (Zhou et al., 2021),

$$E_w = \frac{1}{16}\frac{\rho g H_i \omega L}{k}\left(1 + \frac{2kh}{\sinh 2\,kh}\right) \tag{4}$$

where ρ and g is the density of water and the acceleration of gravity, respectively. H_i is the incident wave height, and ω is the incident wave frequency, L is the transverse length of floater, k is the wave number, and h is the water depth.

In this experiment, the average wave power of the WEC is defined as the power against the total damping forces (including PTO damping F_{pto} and friction damping) as shown in Fig. 7, with the wave power calculated as:

Table 2
Free decay characteristics of different WEC buoys.

Model	Natural period (s)		b_f (kg·s^{-1})
	Exp	Sim	
Rectangle	0.84	0.844	21.4
Tri-baffle	0.87	0.87	54.7

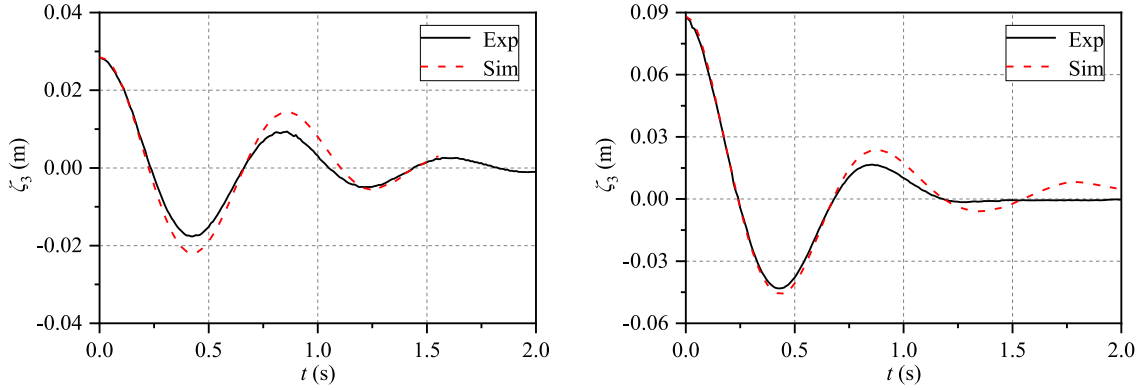

Fig. 6. Free decay curves of the WEC.

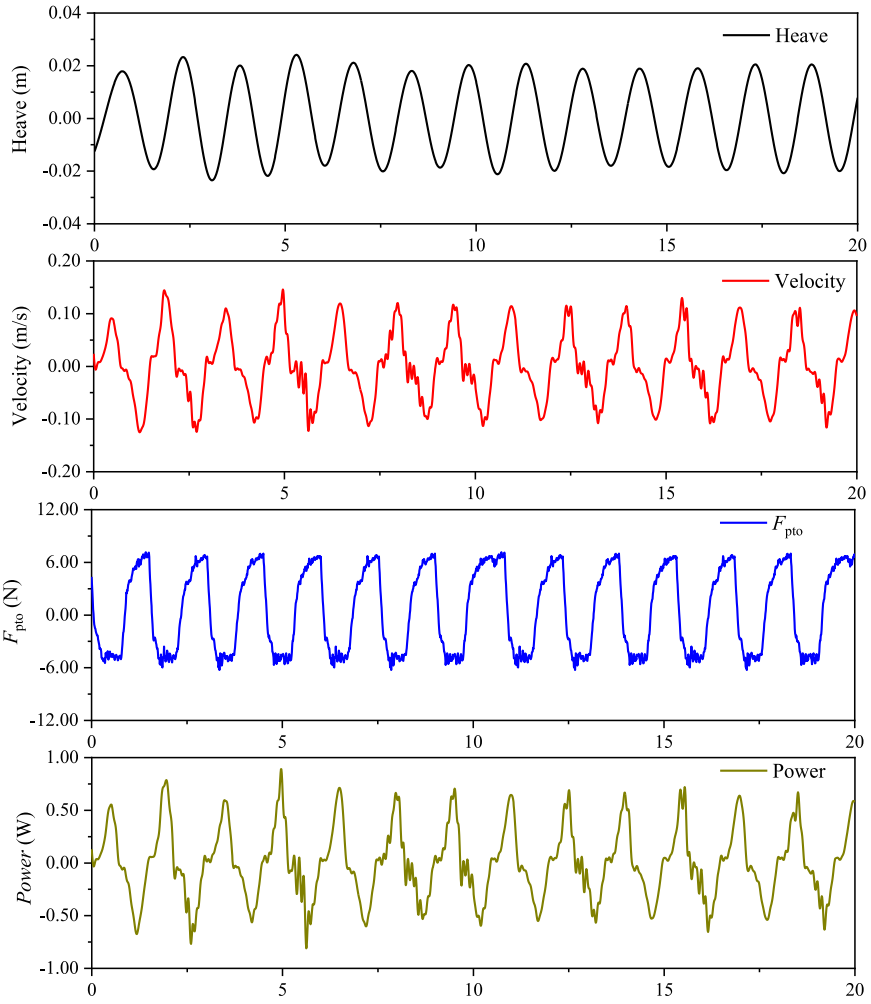

Fig. 7. Time histories of related parameters with $H_i = 0.05$ m and $T = 1.5$ s.

$$P_{ave} = \frac{1}{nT}\int_{t}^{t+nT} \left(F_{pto} \cdot V + b_f \cdot V^2\right) dt \tag{5}$$

where n is the number of stable cycles selected for computation, T is the incident wave period, t is the start time of the calculation, V is the heave motion velocity of the WEC model, which is calculated by differentiating the displacement measured by a linear displacement sensor. F_{pto} is the damping force provided by the PTO system, which can be calculated as follow,

$$F_{pto} = F_1 - m_1(a+g) \tag{6}$$

where F_1 is the data measured by tension pressure sensor, m_1 is the mass of the toothed rack, and a is the acceleration of the WEC buoy, which can be obtained by taking the second derivative of the displacement data.

Additionally, the b_f represents the total friction coefficient, which can be calculated by comparing the experimental and numerical free decay curves and the results are shown in Table 2.

$$b_f = 2\kappa c_0/\omega_0 \tag{7}$$

$$\kappa = \ln[(C_{ai} - T_{ai}) / (C_{ai+1} - T_{ai+1})] / 2\pi \tag{8}$$

where ω_0 is the natural frequency in the heave direction, $c_0 = \rho g A_\omega$ is the hydrostatic restoration coefficient, and A_ω is the wetted surface of the WEC model. The dimensionless damping κ can be determined through a free decay test, where C_{ai}, C_{ai+1}, T_{ai}, and T_{ai+1} are the consecutive crests and troughs of the displacement curve of free decay test, details can be referred to (Zhou et al., 2024b).

The energy conversion efficiency η is defined as the ratio of the average wave energy conversion power P_{ave} to the incident wave power E_w. Considering the variation in the mass of the WECs, the power per unit mass P_m is introduced, the ratio of the average wave energy conversion power P_{ave} and the mass M of the model

$$\eta = P_{ave}/E_w \tag{9}$$

$$P_m = P_{ave}/M \tag{10}$$

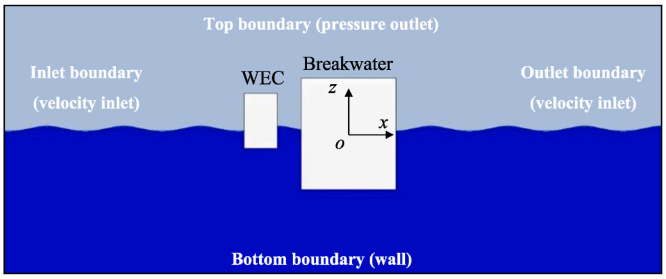

Fig. 8. Diagram of the two-dimensional numerical wave tank model.

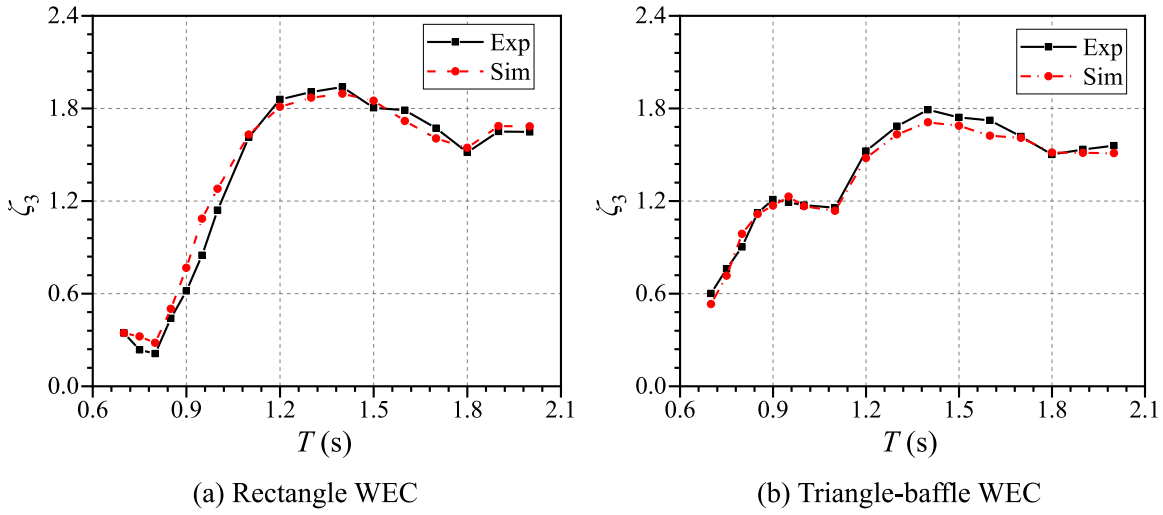

Fig. 9. Comparison of numerical simulation and experimental results.

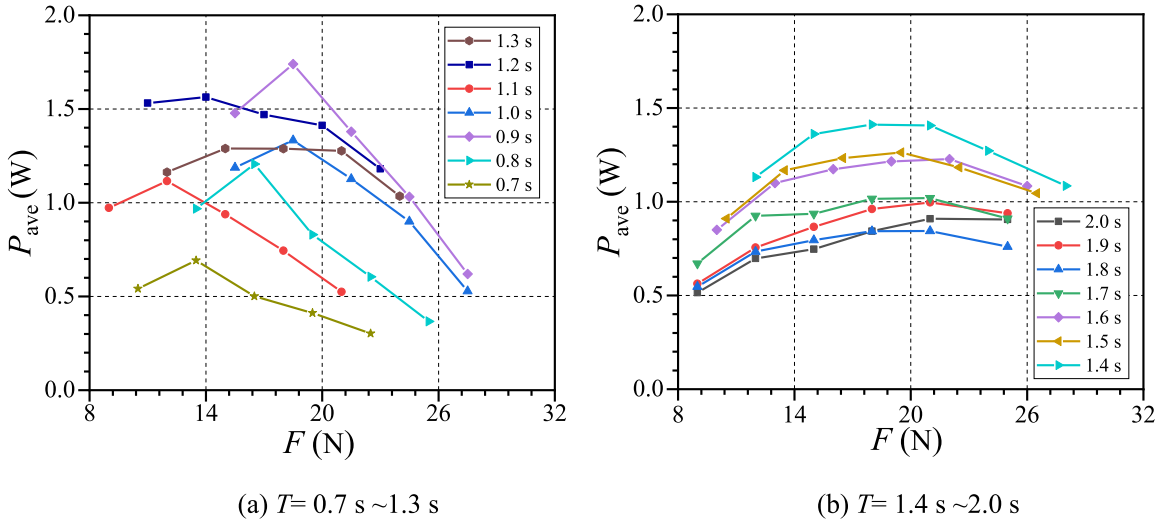

Fig. 10. Average power of the hybrid system with rectangle WEC under different damping force.

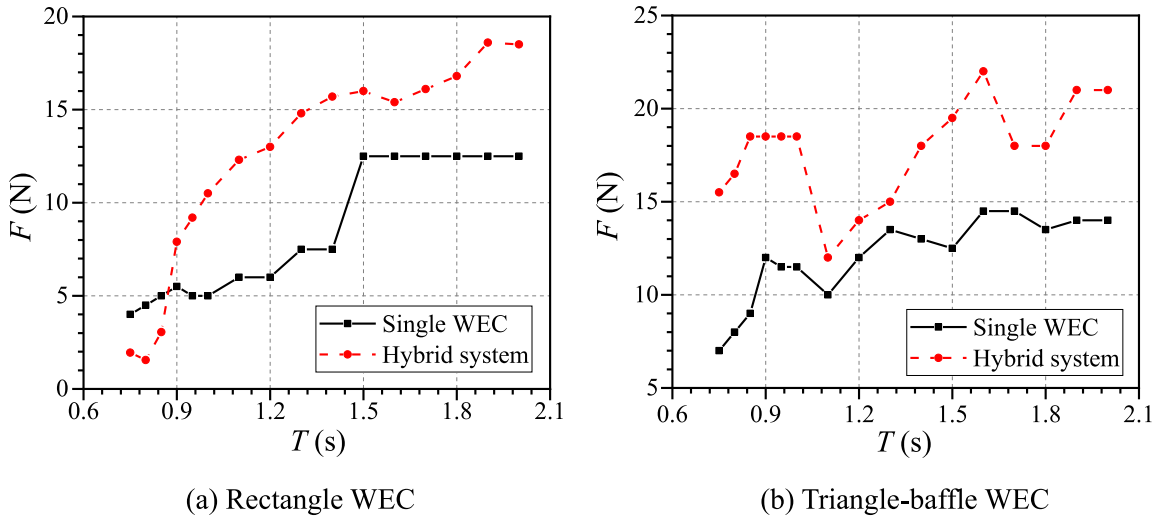

Fig. 11. PTO damping force corresponding to optimal level under different wave period for single WEC and hybrid system.

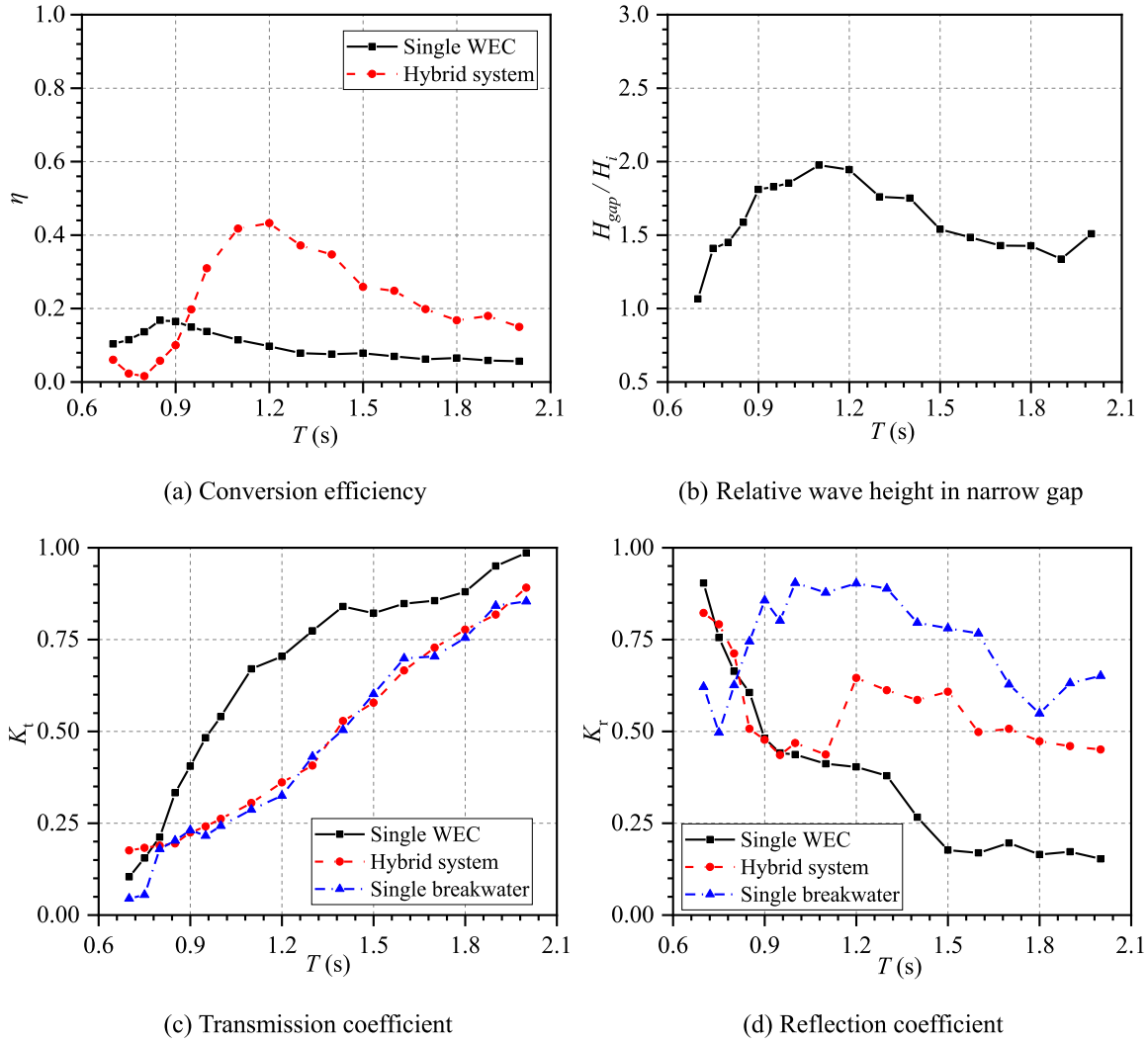

Fig. 12. Variations of η, H_{gap}/H_i, K_t and K_r for single WEC and hybrid system with rectangle WEC.

3. Verification of the experiment

To validate the accuracy of the experimental model and demonstrate the repeatability of the experimental results, a numerical model is developed using the Computational Fluid Dynamics (CFD) method to compare with the experimental results of the hybrid system. As shown in Fig. 8, a quasi-two-dimensional numerical wave flume is established in Star-CCM + software with the width $L_y = 0.01$m in the y direction. The WEC is constrained to move only in the z direction and the breakwater is assumed to be fixed. The Finite Volume Method (FVM) is employed for spatially discretization and the Volume of Fluid (VOF) method (Bilandi et al., 2018) is applied to capture the free surface interface between the air and water phases. The accuracy of the numerical model has been verified in previous studies (Zhang et al., 2020a). Additionally, the frictional damping coefficient b_f obtained through free decay experiment combined with Equations (8) and (9) was incorporated to the numerical model. With no PTO system configured, numerical simulations and physical experiments were conducted for comparative verification (as shown in Fig. 9). The motion responses of both approaches show good consistency (mean relative error <5 %). This validates the accuracy of the determined frictional damping and demonstrates the repeatability of the experiment.

4. Results and discussion

4.1. Determination of the optimal damping level

The Power Take-Off system, serving as a key component of the hybrid system, plays an essential role in energy conversion efficiency (Azam et al., 2024). Therefore, selecting an appropriate PTO damping to maximize the conversion efficiency of the WEC is of critical importance. In this study, the permanent magnet damper can provide a finite number of different values of the PTO damping force by adjusting damping levels. Taking the hybrid system with a rectangle WEC as an example, the average wave powers of the WEC with different PTO damping forces are shown in Fig. 10. The average wave power shows a trend of initial increase followed by a reduction when increasing the damping force. The damping force corresponding to the maximum wave power is taken as the optimal level damping force. Similarly, the PTO damping force corresponding to optimal level for different models are summarized in Fig. 11. Generally, the PTO damping force corresponding to optimal level of all models becoming larger with the wave period. Since the size of single floater becomes relatively small compared to the wavelength when the wave period $T > 1.5$ s, resulting in less noticeable variations in optimal PTO damping. Notably, the PTO damping force corresponding to optimal level for the WEC integrating with the breakwater is generally higher than that of a single WEC, indicating that the integration with a floating breakwater alters the dynamic response of the WEC. The same

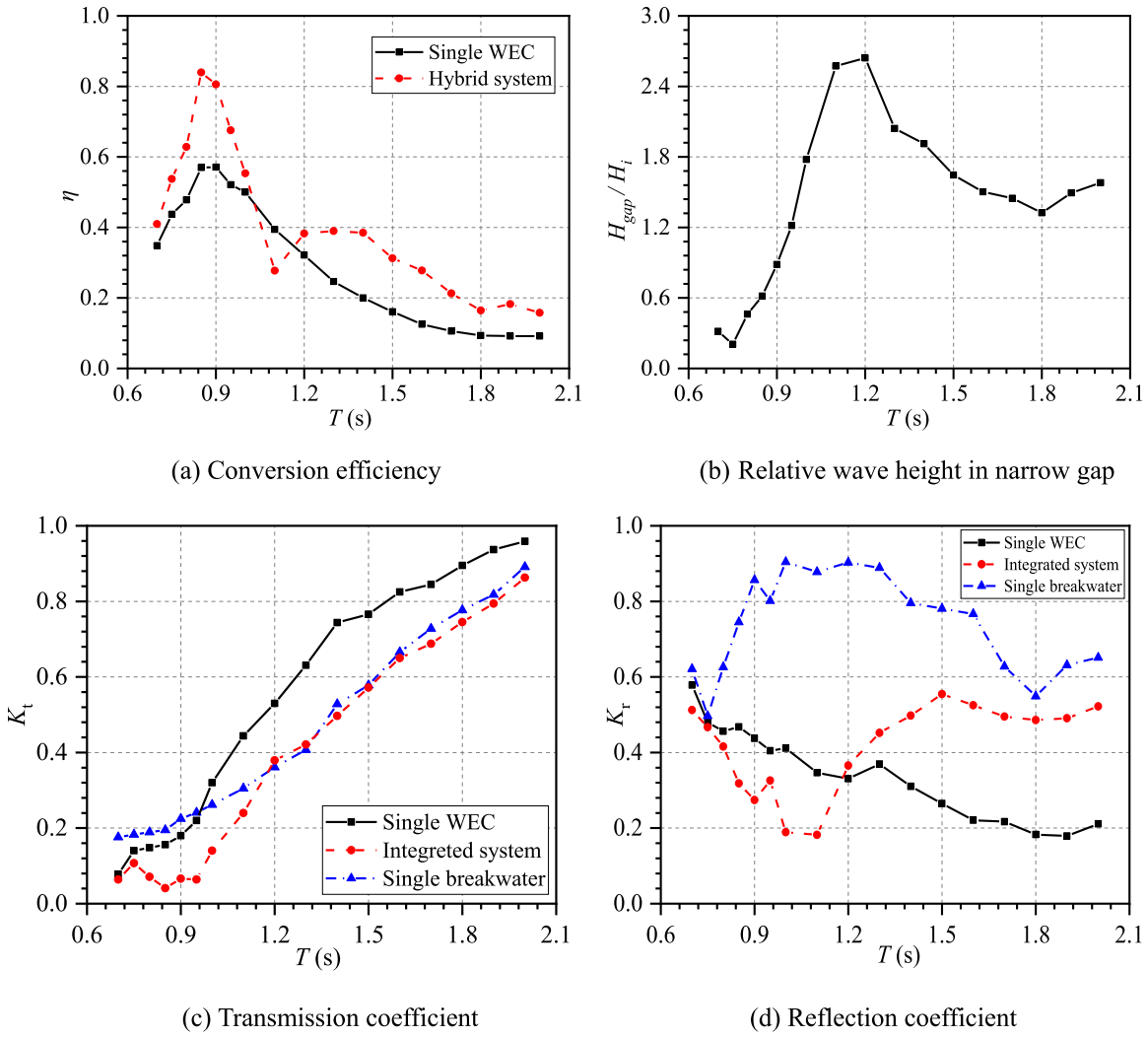

Fig. 13. Variations of η, H_{gap}/H_i, K_t and K_r for single WEC and hybrid system with triangle-baffle WEC.

method was applied to obtain the peak-efficiency damping force for all models in this study. In other words, all results presented were measured under conditions of optimal level PTO damping.

4.2. Performance of the hybrid system with different WECs

This section considered two WEC-breakwater hybrid systems with different geometric configurations (symmetrical rectangular WEC and asymmetrical triangular-baffle WEC) to investigate their wave energy harvesting and attenuation characteristics, while exploring their interaction mechanisms. To eliminate the interference of dimensional differences on hydrodynamic performance, the triangular-baffle floater maintains the same width as the rectangular floater ($B = 0.17$ m), with specific dimensions detailed in Table 1. The gap between the WEC and breakwater was set at $s = 0.055$m. The incident wave height was $H_i = 0.05$ m, and the wave periods T varied from 0.7 s to 2.0 s. Comparative results, including conversion efficiency, narrow-gap wave height coefficients, transmission coefficients, and reflection coefficients, are shown in Figs. 12 and 13.

Figs. 12(a) and Fig. 13 (a) depict the variation of wave energy conversion efficiency for hybrid systems with varying WEC geometries and their corresponding single WEC. As depicted in Fig. 12(a), the wave energy conversion efficiency of the hybrid system with a symmetrical rectangle WEC initially becomes larger with the wave period and peaks at $T = 1.2$ s, where it reaches a maximum of 43.2 %, which represents a 1.57-times increase compared to the single rectangle WEC. This enhancement is primarily driven by the narrow-gap resonance of the hybrid system with rectangle WEC. When the incident wave period matches the natural frequency of the gap ($T = 1.2$ s), the motion of rectangle WEC is amplified due to resonance, generating strong radiated waves. However, the conversion efficiency for the hybrid system is lower compared with the single WEC when $T < 0.9$ s, suggesting that integration between the WEC and floating breakwater is detrimental to the performance of the symmetrical rectangle WEC at lower frequencies. Fig. 13 (a) illustrates the wave energy conversion efficiency of the hybrid system with an asymmetrical triangle-baffle WEC. Both the single and the hybrid systems with asymmetric WEC exhibit enhanced power generation capabilities, achieving peak values of 57.1 % for the single WEC and 83.9 % for the hybrid system. Distinct from the symmetric WEC, the hybrid system with asymmetrical triangle-baffle WEC demonstrates improved energy conversion efficiency not only at peak values but also at lower frequencies, indicating a broader energy capture capability. Further comparative analysis of Figs. 12(a) and Fig. 13 (a) indicates that the asymmetrical triangle-baffle WEC hybrid system outperforms the symmetrical rectangle WEC system, with peak efficiency nearly twice as high. The rectangle WEC benefits from the narrow-gap resonance at $T = 1.2$ s, where the wave amplitude in the narrow gap is maximized, as shown in Fig. 12(b). This resonance enhances the wave energy available for conversion, leading to peak efficiency. In contrast, the triangle-baffle WEC, while also experiencing

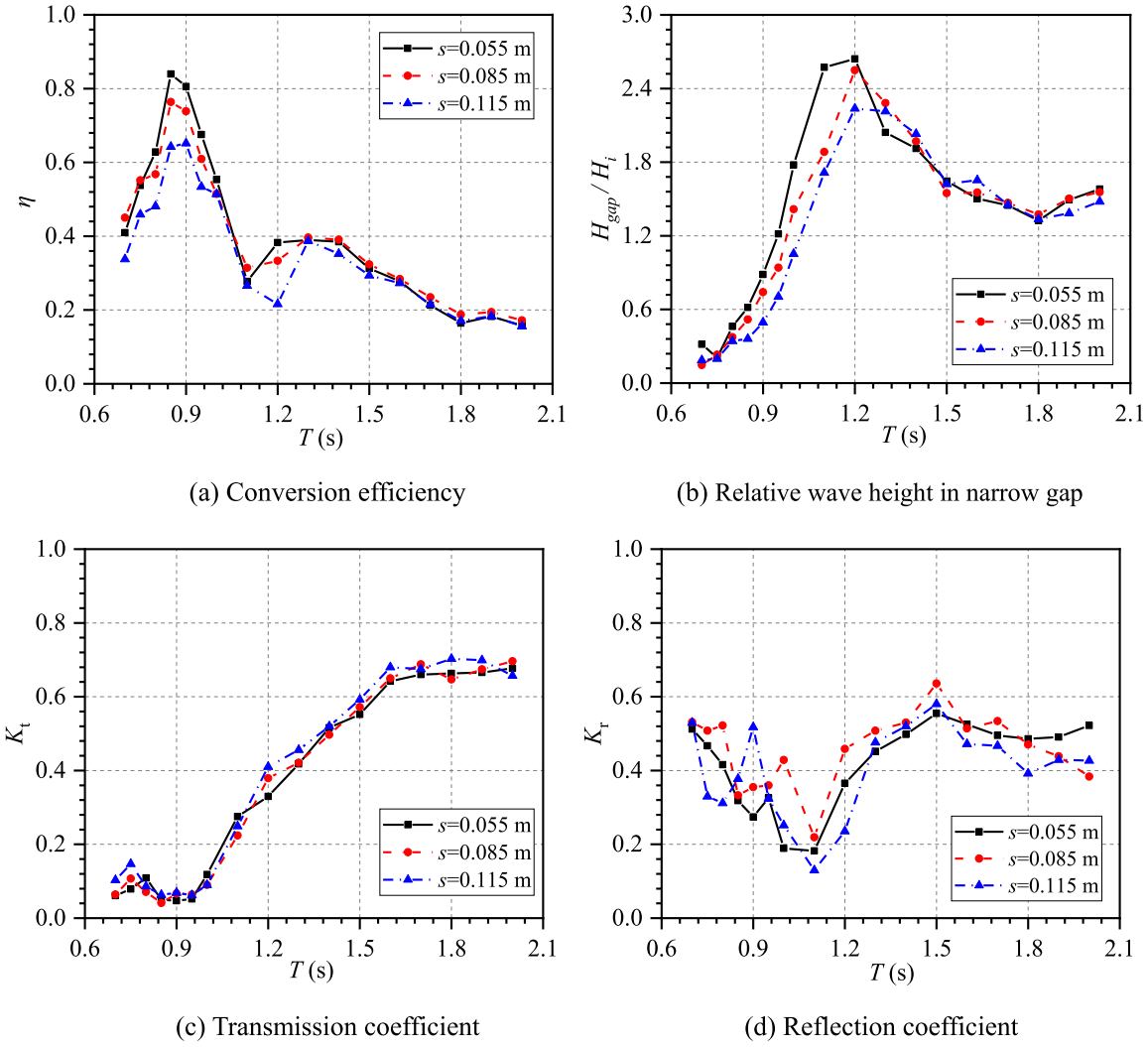

Fig. 14. Variations of η, H_{gap}/H_i, K_t and K_r for hybrid system with different gap widths.

narrow-gap resonance at $T = 1.2$ s as indicated by the increased wave height in Fig. 13, does not exhibit the same efficiency peak. This difference in performance may be attributable to the geometric symmetry of the WEC. In the hybrid system with rectangle WEC, the symmetrical shape of the WEC enables equivalent wave absorption capabilities in both the incident and reflected directions (Zhang et al., 2021a). Therefore, the gap resonance improves its wave extraction performance. In contrast, the asymmetric triangular baffle configuration exhibits a weaker ability to absorb reflected waves. Thus, part of the wave energy was trapped in the gap when gap resonance occurs, resulting in the reduction of the wave power.

Fig. 12(c)–(d) and Fig. 13(c) and (d) present the transmission and reflection coefficients for the single WEC, the single breakwater, and the integrated WEC-breakwater system for further analysis of the hydrodynamic parameters. Overall, the transmission coefficient exhibits an upward trend with an increasing wave period, while the reflection coefficient demonstrates a declining trend. Fig. 12(c) shows the transmission coefficient of the rectangular WEC hybrid system is very close to that of the single breakwater. In contrast, the triangular baffle WEC hybrid system shown in Fig. 13 demonstrates significant advantages in short-wave attenuation, with a maximum reduction of 71 %. This difference can be explained by the higher conversion efficiency of the asymmetric triangular baffle WEC at low frequencies, meaning that much wave energy is absorbed and thus less wave energy is transmitted. This shows that asymmetric WEC not only has a higher energy conversion efficiency, but also optimizes the performance of the breakwater. As depicted in Figs. 12(d) and 13(d), the hybrid system exhibits a reduction in reflection coefficient relative to the standalone breakwater. This is because the WEC positioned in front of the breakwater absorbs part of the energy reflected by the breakwater, thereby reducing the reflection coefficient. Moreover, this reduction in reflection is particularly pronounced during the occurrence of narrow-gap resonance since the wave energy is confined to the narrow gap.

In summary, the integration of WEC and breakwater enhances its capabilities for wave energy absorption and attenuation. The asymmetric triangle-baffle WEC-breakwater hybrid system with an exhibits a broader efficiency range frequency, as well as an improvement in attenuation of short waves. The impact of narrow-gap resonance on the performance of the hybrid system depends on the shape of the WEC, symmetrical WECs benefit, but asymmetrical ones exhibit the opposite effect.

4.3. *Influence of narrow gap width*

The gap width significantly influences the narrow-gap resonance and the performance of the OB-type WEC-floating breakwater system. Three models with different widths of narrow gap ($S = 0.055$ m, $S = 0.085$ m, $S = 0.115$ m) were comparative analyzed for further elucidation of the influence of narrow gap width. Fig. 14(a) shows that the impacts of narrow gap width on the conversion efficiency of the hybrid system is

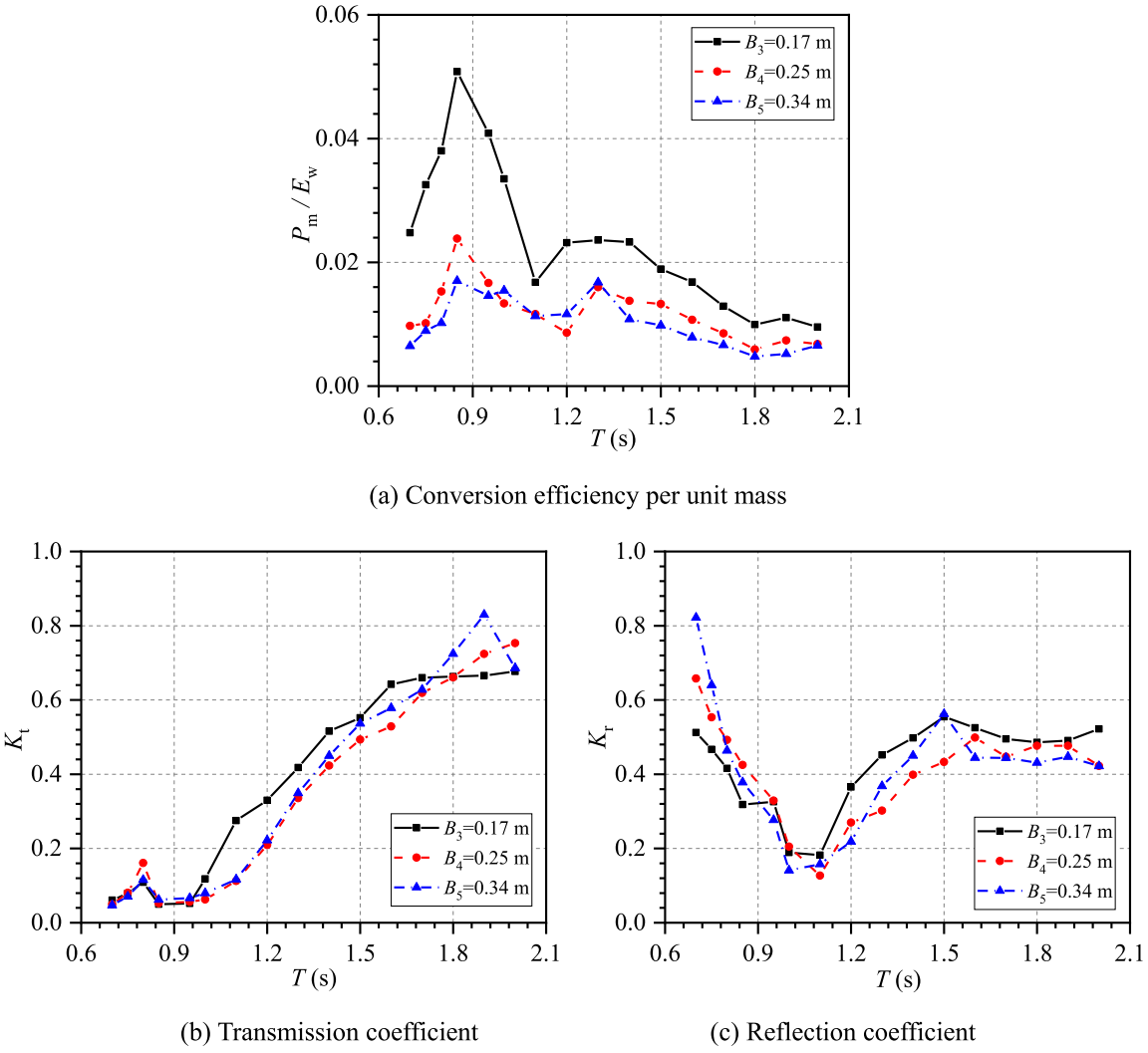

Fig. 15. Variations of η, H_{gap}/H_i, K_t and K_r for hybrid system with different WEC widths.

primarily observed in short waves. This is because the longer waves are less reflected by the floating breakwater and tend to be transmitted through. With the increase in narrow gap width, there is a decrease in the conversion efficiency of the WEC, with peak values being 83.9 %, 76.3 %, and 64.2 % respectively. Fig. 14(b) shows the wave height within the narrow gap reduces when increasing gap width, due to the reduced energy accumulation effect from the increased water volume in the gap. The transmission coefficients of hybrid systems with different gap widths are slightly different, as shown in Fig. 14(c). Fig. 14(d) indicates the phenomenon of narrow-gap wave resonance as evidenced by the reflection coefficient attaining its minimum value at the same time, confirming that most of the energy is concentrated in the narrow gap. Results in Fig. 14 recommended that the WEC should be positioned as close as possible to the breakwater within a hybrid system to better harness wave energy.

4.4. Influence of WEC width

To improve the wave energy harvesting and attenuation capabilities of the hybrid system, the width of the WEC is an important parameter that requires optimization. This section investigated the hydrodynamic performance of the triangle-baffle WEC-breakwater hybrid system with varying widths. The details of the model dimensional parameters are shown in Table 1, three different WEC widths (0.17 m, 0.25 m, 0.34 m) are selected. Other parameters are consistent with those of Section 4.2, and the narrow gap width is set at $S = 0.055$ m.

Due to the varying masses of the models, Fig. 15 additionally presents the results of conversion efficiency per unit mass P_m/E_w, transmission coefficient K_t and reflection coefficient K_r. Fig. 15(a) shows the energy conversion efficiency per unit mass of the hybrid system exhibits a significant decrease with the increase of the WEC width, with the narrow configuration ($B_3 = 0.17$ m) demonstrating better performance under short-wave conditions. The reason is that the resonance period of the narrow gap matches the short-wave period, generating resonance enhancement effects that significantly improve energy capture capability; wider WEC may experience intensified surface flow separation, forming larger-scale vortex structures that dissipate more energy. As the wave period increases, differences in energy conversion efficiency per unit mass between hybrid system with varying WEC widths gradually towards consistency. Fig. 15(b) shows the transmission coefficient of the hybrid system reduces when increasing the WEC width, which indicates that the hybrid system with a wider WEC shows better wave attenuation performance. Fig. 15(c) show the influence of WEC width on the reflection coefficient is related to the wave periods. The reflection coefficient reduces with the increment of WEC width when $T > 1.2$ s since the narrower WEC has a larger bottom slope and leads to stronger reflection ability. However, during shorter wave periods ($T < 1.2$ s), the narrow WEC exhibits a higher wave absorption capacity, leading to a reduction in reflected energy. These results show that a narrower WEC should be adopted for integration with a breakwater to achieve superior

power generation performance, although with a slight deterioration in wave attenuation performance.

5. Conclusions

In this paper, the hydrodynamic performance of the OB-type WEC-floating breakwater hybrid system is systematically studied via a series of model experiments. The comparative analysis of hybrid systems with different WEC geometries revealed significant performance variations, while the narrow-gap resonance phenomenon and its impacts on system efficiency were thoroughly examined. Key parameters including PTO damping, narrow gap width, and WEC dimensions were optimized. The main findings are summarized as follows:

(1) Integrating the OB-type WEC with a floating breakwater substantially enhances wave energy absorption and attenuation performance. The hybrid system with an asymmetric triangular-baffle WEC outperformed the system with a symmetric rectangular configuration, demonstrating broader operational bandwidth and superior short-wave attenuation capabilities.
(2) Narrow-gap resonance critically influences the energy conversion efficiency of the hybrid system, with distinct effects dependent on WEC geometry. Hybrid system with symmetrical WEC benefit from this phenomenon, whereas asymmetrical WEC designs exhibit adverse responses.
(3) Increasing the narrow gap width between the floating breakwater and the WEC does not compromise the wave attenuation performance of the integrated system but reduces the energy conversion efficiency of the WEC. Additionally, narrower WEC achieve higher conversion efficiency per unit mass, making them more cost-effective.

The limitation of this paper is that the performance of the hybrid system under regular waves is considered, neglecting the behavior of the hybrid system in actual irregular waves. Furthermore, safety assessments of the hybrid systems under extreme sea conditions should be considered.

CRediT authorship contribution statement

Binzhen Zhou: Writing – review & editing, Supervision, Funding acquisition, Conceptualization. **Chusen Lin:** Writing – original draft, Investigation. **Xu Huang:** Writing – review & editing, Investigation. **Qi Zhang:** Writing – review & editing. **Yuan Yuming:** Writing – review & editing. **Hengming Zhang:** Writing – review & editing, Investigation, Data curation, Conceptualization. **Peng Jin:** Writing – review & editing. **Yifeng Yang:** Writing – review & editing.

Declaration of competing interest

The authors declare that they have no known competing financial interests or personal relationships that could have appeared to influence the work reported in this paper.

Acknowledgement

This work is supported by the National Key R & D Program of China (2023YFB4204101), the National Natural Science Foundation of China (52222109, 52201322), Project of State Key Laboratory of Subtropical Building and Urban Science (2023ZB14), Guangdong Basic and Applied Basic Research Foundation (2022B1515020036, 2023A1515012144). The authors of this paper declare that we have no known competing financial interests or personal relationships that could have appeared to influence the work reported in this paper.

References

Astariz, S., Iglesias, G., 2015. The economics of wave energy: a review. Renew. Sustain. Energy Rev. 45, 397–408. https://doi.org/10.1016/j.rser.2015.01.061.
Azam, A., Ahmed, A., Yi, M., Zhang, Z., Zhang, Z., Aslam, T., Mugheri, S.A., Abdelrahman, M., Ali, A., Qi, L., 2024. Wave energy evolution: knowledge structure, advancements, challenges and future opportunities. Renew. Sustain. Energy Rev. 205, 114880. https://doi.org/10.1016/j.rser.2024.114880.
Bilandi, R.N., Jamei, S., Roshan, F., Azizi, M., 2018. Numerical simulation of vertical water impact of asymmetric wedges by using a finite volume method combined with a volume-of-fluid technique. Ocean Eng. 160, 119–131. https://doi.org/10.1016/j.oceaneng.2018.04.043.
Chen, Q., Zang, J., Birchall, J., Ning, D., Zhao, X., Gao, J., 2020. On the hydrodynamic performance of a vertical pile-restrained WEC-type floating breakwater. Renew. Energy 146, 414–425. https://doi.org/10.1016/j.renene.2019.06.149.
Cheng, Y., Fu, L., Dai, S., Collu, M., Cui, L., Yuan, Z., Incecik, A., 2022a. Experimental and numerical analysis of a hybrid WEC-breakwater system combining an oscillating water column and an oscillating buoy. Renew. Sustain. Energy Rev. 169, 112909. https://doi.org/10.1016/j.rser.2022.112909.
Cheng, Y., Fu, L., Dai, S., Collu, M., Ji, C., Yuan, Z., Incecik, A., 2022b. Experimental and numerical investigation of WEC-type floating breakwaters: a single-pontoon oscillating buoy and a dual-pontoon oscillating water column. Coast. Eng. 177, 104188. https://doi.org/10.1016/j.coastaleng.2022.104188.
Goda, Y., Suzuki, Y., Port, M.H.D., 1976. Estimation of incident and reflected waves in random wave experiments. https://doi.org/10.1061/9780872620834.048.
Gong, S., Gao, J., Song, Z., Shi, H., Liu, Y., 2024. Hydrodynamics of fluid resonance in a narrow gap between two boxes with different breadths. Ocean Eng. 311, 118986. https://doi.org/10.1016/j.oceaneng.2024.118986.
Gong, S., Gao, J., Yan, M., Song, Z., Shi, H., 2025. Effects of floater motion on wave loads during steady-state gap resonance occurring between two non-identical boxes. Ocean Eng. 323, 120649. https://doi.org/10.1016/j.oceaneng.2025.120649.
He, F., Huang, Z., Law, A.W.-K., 2013. An experimental study of a floating breakwater with asymmetric pneumatic chambers for wave energy extraction. Appl. Energy 106, 222–231. https://doi.org/10.1016/j.apenergy.2013.01.013.
Jiang, S.-C., Bai, W., Cong, P.-W., Yan, B., 2019. Numerical investigation of wave forces on two side-by-side non-identical boxes in close proximity under wave actions. Mar. Struct. 63, 16–44. https://doi.org/10.1016/j.marstruc.2018.08.007.
Jiang, S.-C., Bai, W., Tang, G.-Q., 2018. Numerical simulation of wave resonance in the narrow gap between two non-identical boxes. Ocean Eng. 156, 38–60. https://doi.org/10.1016/j.oceaneng.2018.02.055.
Li, Y., Zhang, C., 2016. Analysis of wave resonance in gap between two heaving barges. Ocean Eng. 117, 210–220. https://doi.org/10.1016/j.oceaneng.2016.03.042.
Madhi, F., Sinclair, M.E., Yeung, R.W., 2014. The "Berkeley Wedge": an asymmetrical energy-capturing floating breakwater of high performance. Marine Systems & Ocean Technology 9, 5–16. https://doi.org/10.1007/BF03449282.
Madhi, F., Yeung, R.W., 2018. On survivability of asymmetric wave-energy converters in extreme waves. Renew. Energy 119, 891–909. https://doi.org/10.1016/j.renene.2017.07.123.
Martinelli, L., Ruol, P., Favaretto, C., 2016. Hybrid structure combining a wave energy converter and a floating breakwater. Proc. Int. Offshore Polar Eng. Conf. ISOPE-I-16-434.
McCartney, B.L., Asce, M., 1985. Floating breakwater design. J. Waterw. Port, Coast. Ocean Eng. 111, 304–318. https://doi.org/10.1061/(ASCE)0733-950X(1985)111:2(304.
Mi, C., Gao, J., Song, Z., Liu, Y., 2025a. Hydrodynamic wave forces on two side-by-side barges subjected to nonlinear focused wave groups. Ocean Eng. 317, 120056. https://doi.org/10.1016/j.oceaneng.2024.120056.
Mi, C., Gao, J., Song, Z., Yan, M., 2025b. Gap resonance between a stationary box and a vertical wall induced by transient focused wave groups. China Ocean Eng. 1–14. https://doi.org/10.1007/s13344-025-0081-y.
Mustapa, M.A., Yaakob, O.B., Ahmed, Y.M., Rheem, C.-K., Koh, K.K., Adnan, F.A., 2017. Wave energy device and breakwater integration: a review. Renew. Sustain. Energy Rev. 77, 43–58. https://doi.org/10.1016/j.rser.2017.03.110.
Ning, D., Zhao, X., Göteman, M., Kang, H., 2016. Hydrodynamic performance of a pile-restrained WEC-type floating breakwater: an experimental study. Renew. Energy 95, 531–541. https://doi.org/10.1016/j.renene.2016.04.057.
Ning, D., Zhao, X., Zhao, M., Kang, H., 2018a. Experimental investigation on hydrodynamic performance of a dual pontoon–power take-off type wave energy converter integrated with floating breakwaters. Proc. IME M J. Eng. Marit. Environ. 233, 991–999. https://doi.org/10.1177/1475090218804677.
Ning, D., Zhu, Y., Zhang, C., Zhao, M., 2018b. Experimental and numerical study on wave response at the gap between two barges of different draughts. Appl. Ocean Res. 77, 14–25. https://doi.org/10.1016/j.apor.2018.05.010.
Ning, D., Zhao, X., Zhao, M., Hann, M., Kang, H., 2017. Analytical investigation of hydrodynamic performance of a dual pontoon WEC-type breakwater. Appl. Ocean Res. 65, 102–111. https://doi.org/10.1016/j.apor.2017.03.012.
Reabroy, W., Ruol, P., Favaretto, C., 2018. Performance analysis of dual-floater systems for wave energy conversion and wave attenuation. Proc. Int. Offshore Polar Eng. Conf.
Zhang, H., Zhou, B., Vogel, C., Willden, R., Zang, J., Geng, J., 2020a. Hydrodynamic performance of a dual-floater hybrid system combining a floating breakwater and an oscillating-buoy type wave energy converter. Appl. Energy 259, 114212. https://doi.org/10.1016/j.apenergy.2019.114212.
Zhang, H., Zhou, B., Vogel, C., Willden, R., Zang, J., Zhang, L., 2020b. Hydrodynamic performance of a floating breakwater as an oscillating-buoy type wave energy

converter. Appl. Energy 257, 113996. https://doi.org/10.1016/j.apenergy.2019.113996.
Zhang, H., Zhou, B., Zang, J., Vogel, C., Fan, T., Chen, C., 2021a. Effects of narrow gap wave resonance on a dual-floater WEC-breakwater hybrid system. Ocean Eng. 225, 108762. https://doi.org/10.1016/j.oceaneng.2021.108762.
Zhang, H., Zhou, B., Zang, J., Vogel, C., Jin, P., Ning, D., 2021b. Optimization of a three-dimensional hybrid system combining a floating breakwater and a wave energy converter array. Energy Convers. Manag. 247, 114717. https://doi.org/10.1016/j.enconman.2021.114717.
Zhang, Y., Zhao, Y., Sun, W., Li, J., 2021. Ocean wave energy converters: technical principle, device realization, and performance evaluation. Renew. Sustain. Energy Rev. 141, 110764. https://doi.org/10.1016/j.rser.2021.110764.
Zhao, W., Taylor, P.H., Wolgamot, H.A., Molin, B., Eatock, T.R., 2020. Group dynamics and wave resonances in a narrow gap: modes and reduced group velocity. J. Fluid Mech. 883, A22. https://doi.org/10.1017/jfm.2019.879.
Zhao, X., Ning, D., Zhang, C., Kang, H., 2017a. Hydrodynamic investigation of an oscillating buoy wave energy converter integrated into a pile-restrained floating breakwater. Energies 10, 712. https://doi.org/10.3390/en10050712.
Zhao, X., Ning, D., Zhang, C., Kang, H., Liu, Y., 2017b. Analytical study on an oscillating buoy wave energy converter integrated into a fixed box-type breakwater. Math. Probl Eng. 1, 1–9. https://doi.org/10.1155/2017/3960401.
Zhao, X.L., Ning, D.Z., Liang, D.F., 2019a. Experimental investigation on hydrodynamic performance of a breakwater-integrated WEC system. Ocean Eng. 171, 25–32. https://doi.org/10.1016/j.oceaneng.2018.10.036.
Zhao, X.L., Ning, D.Z., Zou, Q.P., Qiao, D.S., Cai, S.Q., 2019b. Hybrid floating breakwater-WEC system: a review. Ocean Eng. 186, 106126. https://doi.org/10.1016/j.oceaneng.2019.106126.
Zhou, B.Z., Li, J.H., Zhang, H.M., Chen, L.F., Wang, L., Jin, P., 2021. Wave extraction and attenuation performance of an Edinburgh Duck wave energy converter. China Ocean Eng. 35 (6), 905–913. https://doi.org/10.1007/s13344-021-0079-z.
Zhou, B., Hu, J., Jin, P., Sun, K., Li, Y., Ning, D., 2023a. Power performance and motion response of a floating wind platform and multiple heaving wave energy converters hybrid system. Energy 265, 126314. https://doi.org/10.1016/j.energy.2022.126314.
Zhou, B., Hu, J., Wang, Y., Jin, P., Jing, F., Ning, D., 2023b. Coupled dynamic and power generation characteristics of a hybrid system consisting of a semi-submersible wind turbine and an array of heaving wave energy converters. Renew. Energy 214, 23–38. https://doi.org/10.1016/j.renene.2023.06.013.
Zhou, B., Huang, X., Lin, C., Zhang, H., Peng, J., Nie, Z., Jin, P., 2024a. Experimental study of a WEC array-floating breakwater hybrid system in multiple-degree-of-freedom motion. Appl. Energy 371, 123694. https://doi.org/10.1016/j.apenergy.2024.123694.
Zhou, B., Lin, C., Huang, X., Zhang, H., Zhao, W., Zhu, S., Jin, P., 2024b. Experimental study on the hydrodynamic performance of a multi-DOF WEC-type floating breakwater. Renew. Sustain. Energy Rev. 202, 114694. https://doi.org/10.1016/j.rser.2024.114694.
Zhou, B., Wang, Y., Zheng, Z., Jin, P., Ning, D., 2023c. Power generation and wave attenuation of a hybrid system involving a heaving cylindrical wave energy converter in front of a parabolic breakwater. Energy 282, 128364. https://doi.org/10.1016/j.energy.2023.128364.
Zhou, B., Zhang, Q., Hu, J., Jin, P., Zhang, H., Zheng, S., 2023d. Power performance of an asymmetric wave energy converter near a partial reflection wall. Ocean Eng. 280, 114634. https://doi.org/10.1016/j.oceaneng.2023.114634.
Zhou, B., Zhang, Q., Jin, P., Li, Y., Liu, Y., Zheng, S., Ning, D., 2022a. Geometric asymmetry in the energy conversion and wave attenuation of a power-take-off-integrated floating breakwater. Ocean Eng. 246, 110576. https://doi.org/10.1016/j.oceaneng.2022.110576.
Zhou, B., Zheng, Z., Jin, P., Wang, L., Zang, J., 2022b. Wave attenuation and focusing performance of parallel twin parabolic arc floating breakwaters. Energy 260, 125164. https://doi.org/10.1016/j.energy.2022.125164.
Zhou, B., Zheng, Z., Zhang, Q., Jin, P., Wang, L., Ning, D., 2023e. Wave attenuation and amplification by an abreast pair of floating parabolic breakwaters. Energy 271, 127077. https://doi.org/10.1016/j.energy.2023.127077.